Eur. Phys. J. B **42**, 205–217 (2004)
DOI: 10.1140/epjb/e2004-00373-8

THE EUROPEAN PHYSICAL JOURNAL B

Temperature and field dependence of the magnetic properties of $Nd_{2-x}Ce_xCuO_4$

T. Chatterji[1,2,a], K. Siemensmeyer[3], S. Welzel[3], and W. Caliebe[4]

[1] Institut Laue-Langevin, BP 156, 38042 Grenoble Cedex 9, France
[2] Max-Planck-Institut für Physik Komplexer Systeme, Nöthnizerstrasse 38, 01187 Dresden, Germany
[3] Hahn-Meitner-Institut, Glienickerstrasse 100, 14109 Berlin, Germany
[4] Institut für Festkörperforschung, Forschungszentrum Jülich, 52425 Jülich, Germany

Received 9 April 2004
Published online 14 December 2004 –

Abstract. We have investigated the magnetic ordering of $Nd_{2-x}Ce_xCuO_4$ for $x = 0$, 0.09, 0.13, 0.15 and 0.18 by neutron diffraction at low temperatures down to 33 mK and under magnetic field up to 5 tesla applied along $[1, -1, 0]$ crystallographic direction. At zero applied magnetic field Cu magnetic sublattice orders at $T_N \approx 250$, 210, 130 and 105 K for $x = 0$, 0.09, 0.13, 0.15, respectively. No long range magnetic order of the Cu could be detected for $x = 0.18$. The magnetic order of Nd was found in all samples, with a gradual increase of the polarized magnetic moment with decreasing temperature, saturating around 1 K. Hyperfine induced nuclear polarization of the Nd nuclear spin has been observed below about 400 mK for samples with $x = 0$, 0.13, 0.15 and 0.18. Field variation of the intensities of the principal and superstructure reflections of $Nd_{2-x}Ce_xCuO_4$ at millikelvin temperatures shows a field-induced second-order double-**k** to single-**k** phase transition at $H_c = 0.75$ and 0.56 tesla for samples with $x = 0$ and 0.15, respectively at $T = 50$ mK. We have also investigated the polarization of the Nd electronic sublattice due to the field of the Cu sublattice by the element specific X-ray resonant magnetic scattering investigation with synchrotron radiation.

PACS. 75.25.+z Spin arrangements in magnetically ordered materials (including neutron and spin-polarized electron studies, synchrotron-source X-ray scattering, etc.)

1 Introduction

The discovery of superconductivity in electron-doped cuprates [1] $R_{2-x}Ce_xCuO_4$ (R = Ce, Pr, Sm) following the discovery of high temperature superconductivity in hole-doped $La_{2-x}Sr_xCuO_4$ and $RBa_2Cu_3O_{6+x}$ (R = rare earth element) raised the question of 'hole-electron symmetry/asymmetry' in the theory of high temperature superconductivity [2]. This induced a large number of experimental and theoretical investigations on both classes of materials [2]. The magnetic ordering and the spin structures of the parent material Nd_2CuO_4 (space group I4/mmm) of the electron-doped superconductor [1] $Nd_{2-x}Ce_xCuO_4$ have been studied by several authors by neutron diffraction [3–8]. The three-dimensional ordering temperature T_N of Nd_2CuO_4 depends on the oxygen stoichiometry and lies in the temperature range from 245 to 276 K. Below T_N the magnetic moments of the Cu ions order with a propagation vector $\mathbf{k} = (\frac{1}{2}, \frac{1}{2}, 0)$. The magnetic structure of Nd_2CuO_4 has been found to be of non-collinear double-**k** type in which the propagation vectors $\mathbf{k_1} = (\frac{1}{2}, \frac{1}{2}, 0)$ and $\mathbf{k_2} = (\frac{1}{2}, -\frac{1}{2}, 0)$ are coupled. Nd_2CuO_4 undergoes two spin-reorientation phase transitions [3–5] at 75 and 30 K. The Nd magnetic moment is polarized at all temperatures below T_N but the ordering becomes complete at about 1 K. Figure 1 shows the non-collinear double-**k** magnetic structures of Nd_2CuO_4 in phases I, II and III proposed by Lynn and coworkers [4,5] along with the collinear single-**k** structure models reported previously [3]. It is to be noted that collinear single-**k** and and non-collinear double-**k** structures can not be distinguished by neutron diffraction experiments unless they are performed under applied magnetic field or uniaxial stress. The non-collinear double-**k** magnetic structure models of Lynn and coworkers [4,5] have been derived from their neutron diffraction experiments under magnetic field applied along both [110] and [100] crystallographic directions. Below about $T = 400$ mK the nuclear magnetic moments of the ^{143}Nd and ^{145}Nd nuclei of Nd_2CuO_4 become polarized due to the hyperfine field of the ordered Nd electronic moments. We reported the results of nuclear polarization in undoped Nd_2CuO_4 [9]. We also reported [9]

[a] e-mail: chatt@ill.fr
Has changed his surname from "Chattopadhyay" to "Chatterji".

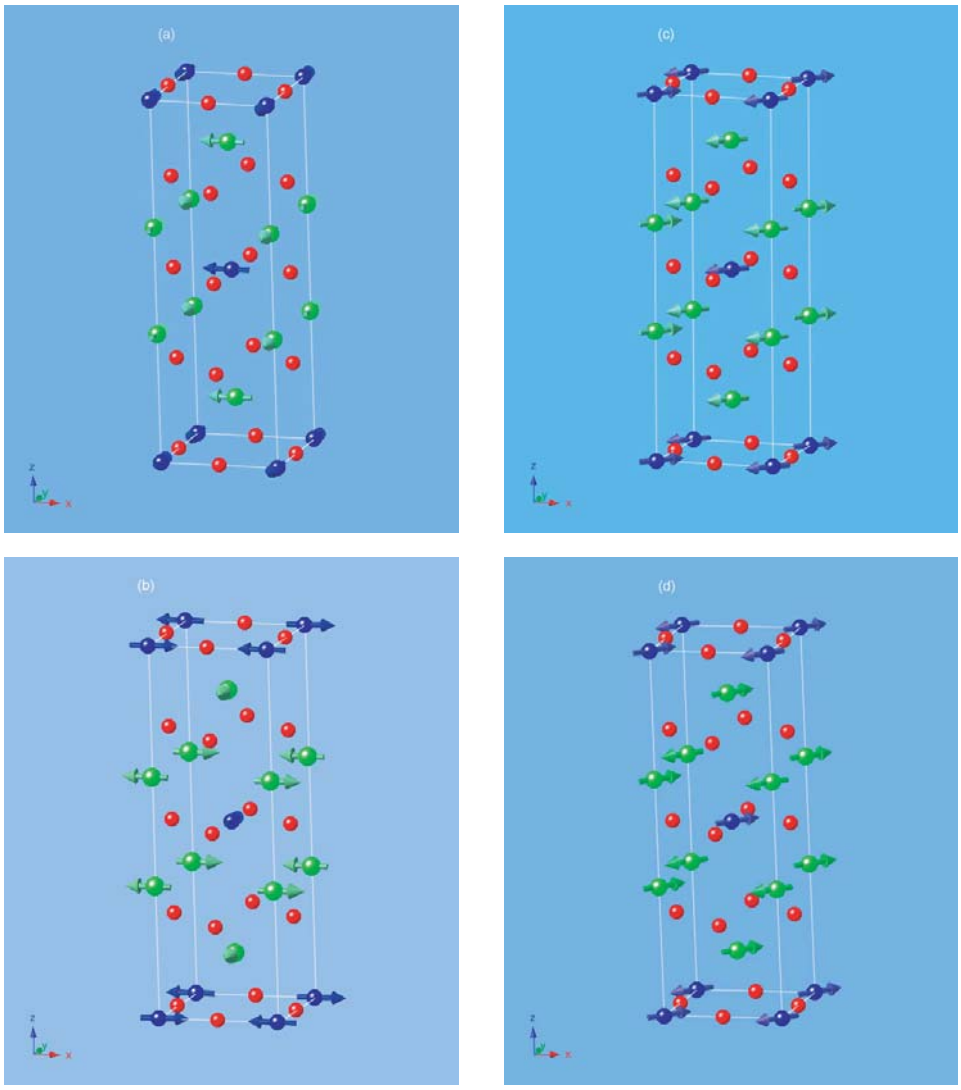

Fig. 1. (a) The non-collinear (double-**k**) magnetic structure models of Nd_2CuO_4 in phases I and III and (b) that in phase II. (c) The corresponding collinear (single-**k**) magnetic structure models of Nd_2CuO_4 in phases I and III and (d) that in phase II. The diffraction patterns of models (a) and (c) and also those of (c) and (d) are indistinguishable unless one applies uniaxial stress or magnetic field. Lynn and coworkers [4,5], based on their field dependent investigations, claim that the non-collinear models (a) and (b) are the correct magnetic structures.

the field-induced double-**k** to single-**k** phase transition on undoped Nd_2CuO_4 at $H_c \approx 0.75$ T at low temperature. We have extended these investigations on doped samples. We report the results of our systematic detailed neutron diffraction investigation of the temperature and field dependence of $Nd_{2-x}Ce_xCuO_4$ down to about 33 mK and up to 5 tesla. We have investigated the polarization of the Nd electronic sublattice by the recently developed element specific X-ray resonant magnetic scattering with synchrotron radiation on the undoped Nd_2CuO_4.

The paper has been organized as follows. In Section 2 experimental details are given. In Section 3.1 we describe the results of zero-field neutron diffraction investigations. In Section 3.2 the neutron diffraction results under magnetic field are described. In Section 4 we describe the results of resonance X-ray magnetic scattering experiments. We discuss the results of the experiments in Section 5. Section 6 gives the summary and conclusions.

2 Experimental

Neutron diffraction experiments were performed on plate-like single crystals of Nd_2CuO_4 and $Nd_{2-x}Ce_xCuO_4$ for $x = 0.13, 0.15$ and 0.18 of varying weights ranging from about 500 mg to about 1 g on the two-axis diffractometer E4 of the Berlin Neutron Scattering Centre (BENSC) using a ^{3}He-^{4}He dilution insert placed inside a vertical cryomagnet. The crystals were fixed on a copper plate attached to the cold tip of the dilution insert with the $[1, -1, 0]$ axis was approximately parallel to the ω-axis of the diffractometer. We have also used an ordinary helium

cryostat for zero field investigations above 1.5 K. Monochromatic neutrons of wavelength 2.4 Å were obtained by using a PG 002 monochromator. The higher order wavelength contamination was suppressed by using a PG 002 filter. The collimation was 40′-open-40′. The mosaic spread of the crystals were less than the resolution of the diffractometer.

X-ray resonant magnetic scattering investigations were performed on pure Nd_2CuO_4 and $Nd_{2-x}Ce_xCuO_4$ for $x = 0.15$ on wiggler beam line W1 of the HASYLAB at DESY in Hamburg. A plate shaped single crystal of size of about $5\times3\times0.2\,mm^3$ was mounted on helium cryostat which was specially designed for medium energy X-rays. The helium cryostat was fixed on the diffractometer with the vertical scattering plane. The diffractometer was equipped with a perfect Si(111) double monochromator.

3 Neutron diffraction investigations

3.1 Zero field investigation

Magnetic ordering of pure Nd_2CuO_4 and $Nd_{2-x}Ce_xCuO_4$ at zero applied magnetic field had been investigated by neutron diffraction by several groups [3–9]. However, we repeated this investigation on our crystals in order to check whether the previous results are reproducible in our crystals. This was important because we used the same crystals or crystals from the same batch for our inelastic neutron scattering investigation of the Nd magnetic excitations [11–13]. To monitor the the Néel temperature T_N and spin reorientation transitions temperatures we measured the temperature variation of $\frac{1}{2}\frac{1}{2}0$, $\frac{1}{2}\frac{1}{2}1$, $\frac{1}{2}\frac{1}{2}2$ and $\frac{1}{2}\frac{1}{2}3$ superstructure reflections of Nd_2CuO_4. Figure 2a shows the temperature variation of the $\frac{1}{2}\frac{1}{2}1$ reflection which starts growing below $T_N \approx 250$ K. The intensity of this reflection increases continuously as the temperature is decreased down to about 100 K below which it saturates before dropping suddenly to a small value at the first spin reorientation transition temperature $T_1 \approx 75$ K. The intensity of this reflection increases slowly below this temperature and finally increases abruptly at the second spin reorientation transition temperature $T_2 \approx 35$ K. So Nd_2CuO_4 has three magnetic phases. The high temperature phase I is stable between T_N and T_1. The intermediate spin oriented phase II is stable in between T_1 and T_2. The low temperature phase III has the same magnetic structure as the phase I. The intensity of the $\frac{1}{2}\frac{1}{2}1$ reflection decreases again due to the polarization of the Nd electronic moments which contribute a negative term to the magnetic structure factor. At $T \approx 10$ K the contribution to the magnetic structure factor due to the polarization of Nd electronic moments becomes equal to that of Cu moments and therefore the intensity of this reflection becomes almost zero. The intensity of the $\frac{1}{2}\frac{1}{2}1$ reflection increases again at lower temperature where the Nd contribution becomes greater than that of Cu. It is to be noted that Nd magnetic sublattice does not show any

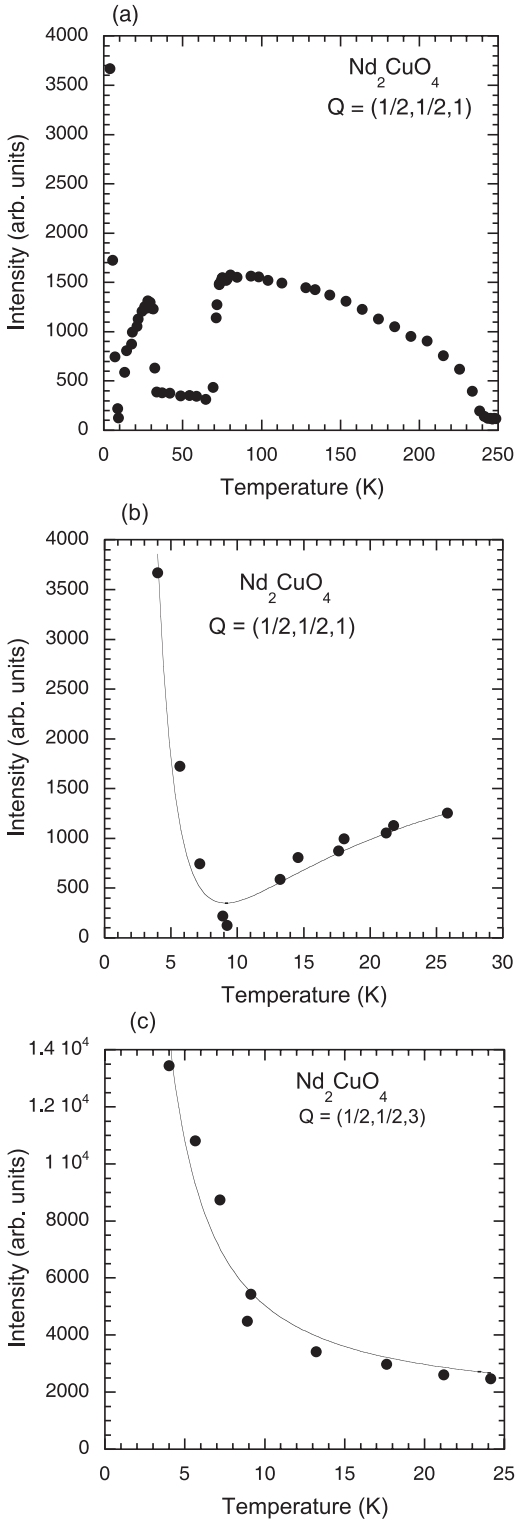

Fig. 2. (a) Temperature variation of the intensity of the $\frac{1}{2}\frac{1}{2}1$ reflection from Nd_2CuO_4. The reflection starts growing below $T_N \approx 250$ K. (b) Temperature variation of the intensity of the $\frac{1}{2}\frac{1}{2}1$ reflection from Nd_2CuO_4 in the temperature range 4–24 K. The continuous curve is the fit of the data with equation (3). (c) Temperature variation of the intensity of the $\frac{1}{2}\frac{1}{2}3$ reflection from Nd_2CuO_4 in the temperature range 4–24 K. The continuous curve is the fit of the data with equation (5).

well defined ordering temperature but rather becomes polarized due to the mean field produced by the Cu magnetic moment. In our X-ray resonant magnetic scattering experiment at the Nd $L_{\rm II}$ absorption edge in which the contribution of the Cu moments is negligible, we have demonstrated this. This will be described in Section 4. Figure 2b shows the temperature variation of the $\frac{1}{2}\frac{1}{2}1$ reflection of Nd_2CuO_4 in the temperature range 4–26 K in the phase III. As we noted previously the intensity of this reflection decreases with decreasing temperature, goes through a minimum at about 10 K and then starts increasing again at lower temperature. We remarked already that this peculiar behaviour is due to the increasing contribution of the Nd magnetic moment at low temperature. We have attempted to fit the temperature variation of the intensity of the $\frac{1}{2}\frac{1}{2}1$ reflection by the following simple model. The intensity of the magnetic Bragg reflection is given by [4]

$$I(\vec{\tau}) = C_1 G(\vec{\tau}) H(\vec{\tau}) \tag{1}$$

where C_1 is a constant. The values of $G(\vec{\tau})$ for $\frac{1}{2}\frac{1}{2}l$ reflections have been tabulated in [4] for $l = 0, 1, \ldots 7$ for the phases I, II, and III. $H(\vec{\tau})$ is also given in the same table. The intensity of the $\frac{1}{2}\frac{1}{2}1$ reflection in phases I and III is given by

$$I = C_1 \times 32.0 \left(f_{\rm Cu}\mu_{\rm Cu} - 1.19 f_{\rm Nd}\mu_{\rm Nd}\right)^2 \tag{2}$$

We assume that the $\mu_{\rm Cu}$ is already saturated below 25 K and $\mu_{\rm Nd}$ increases as Brillouin function or approximately as $\frac{1}{T}$. The form factors $f_{\rm Cu}$ and $f_{\rm Nd}$ are constants for the $\frac{1}{2}\frac{1}{2}1$ reflection. So we can rewrite equation (2) as

$$I = c_1(1 - c_2/T)^2 \tag{3}$$

where $c_1 = C_1(f_{\rm Cu}\mu_{\rm Cu})^2$ and $c_2 = \frac{1.19 f_{\rm Nd}}{f_{\rm Cu}\mu_{\rm Cu}}$. The continuous curve in Figure 2b is the result of the least squares fit of the data with equation (3). Although the fit is not excellent, the temperature variation of the $\frac{1}{2}\frac{1}{2}1$ reflection is reproduced qualitatively. Figure 2c shows the temperature variation of the intensity of the $\frac{1}{2}\frac{1}{2}3$ reflection in the temperature range 4–24 K. The reflection increases monotonically as the temperature is decreased. The intensity of this reflection is given by

$$I = C_1 \times 32.0 \left(f_{\rm Cu}\mu_{\rm Cu} + 1.88 f_{\rm Nd}\mu_{\rm Nd}\right)^2 . \tag{4}$$

Under similar approximations as above equation (4) can be reduced to

$$I = c_1(1 + c_2/T)^2 \tag{5}$$

where $c_1 = C_1(f_{\rm Cu}\mu_{\rm Cu})^2$ and $c_2 = \frac{1.88 f_{\rm Nd}}{f_{\rm Cu}\mu_{\rm Cu}}$. The continuous curve in Figure 2c is the result of the least squares fit of the data with equation (5) and looks reasonable.

We have performed similar experiments on the doped $Nd_{2-x}Ce_xCuO_4$ crystals with $x = 0.09$, 0.13, 0.15 and 0.18. The sample with $x \leq 0.15$ showed Cu magnetic order, with ordering temperature $T_N \approx 210$, 130 and 105 K for $x = 0.09$, 0.13 and 0.15, respectively. No long-range magnetic order could be detected for $x = 0.18$. Induced Nd magnetic order was found in all samples, with a gradual increase of the ordered magnetic moment with decreasing temperature, saturating around 1 K. The temperature variation of the superstructure reflections is very similar. Figure 3 shows the temperature variation of the intensities of $\frac{1}{2}\frac{1}{2}0$, $\frac{1}{2}\frac{1}{2}1$ and $\frac{1}{2}\frac{1}{2}3$ reflections of $Nd_{2-x}Ce_xCuO_4$ for $x = 0.13$ as a representative example. The Néel temperature or the Cu ordering temperature of $Nd_{2-x}Ce_xCuO_4$ decreases continuously with doping (Fig. 4). The spin reorientation transitions take place for the doped samples for $x \leq 0.15$. The transition temperatures T_N, T_1 and T_2 are shifted to lower temperatures and the width of the stability range of the intermediate spin reoriented phase (called phase II) is also decreased. For example for the sample with $x = 0.13$ the spin reorientation transition temperatures are $T_1 \approx 10$ K and $T_2 \approx 4$ K. These results are in agreement with those of reference [4].

During the early days of the neutron diffraction investigation of Nd_2CuO_4 it had been noticed by several authors that the intensity of the $\frac{1}{2}\frac{1}{2}0$ reflection which is zero in the low temperature phase below about 30 K starts to increase again below about 400 mK. No satisfactory explanation of this phenomenon was provided before we demonstrated [9] that this increase in intensity can be interpreted as due to the hyperfine induced polarization of the Nd nuclear moments. In fact we demonstrated that the intensities of all superstructure reflections increase with decreasing temperature due to the nuclear polarization. We have extended these measurements on $Nd_{2-x}Ce_xCuO_4$ for $x = 0.13$, 0.15 and 0.18. We have measured temperature variation of the intensities of several nuclear and superstructure reflections. We reported [9] the temperature variation of the intensities of the superstructure reflections of Nd_2CuO_4 at millikelvin temperatures. All superstructure reflections increase in intensity below about 400 mK. The $\frac{1}{2}\frac{1}{2}0$ reflection which has zero intensity in the low temperature magnetic phase below 30 K develops below about 400 mK and grows in intensity down to 33 mK, the lowest temperature obtained during the measurements. None of these reflections shows any sign of saturation down to 33 mK. The intensities of all superstructure reflections of $Nd_{2-x}Ce_xCuO_4$ increase as in the undoped compound.

The cross section for a coherent scattering process in a ordered magnetic material containing polarised nuclei for the case of unpolarised neutron is given by

$$\frac{\sigma_c}{4\pi} = b_c^2 + \left|\frac{r_e\gamma}{2}\mathbf{M}_\perp + \frac{1}{2}b_N\mathbf{IP}\right|^2 \tag{6}$$

where

$$b_N = \frac{2b_i}{\sqrt{I(I+1)}} \tag{7}$$

b_c and b_i are the coherent and incoherent scattering lengths, $\frac{r_e\gamma}{2} = 2.696 \times 10^{-13}$ cm per μ_B is the magnetic scarttering length, r_e is the classical radius of electron, γ is gyromagnetic ratio of the neutron, $\mathbf{M}_\perp = \mu_\perp f(\mathbf{Q})$,

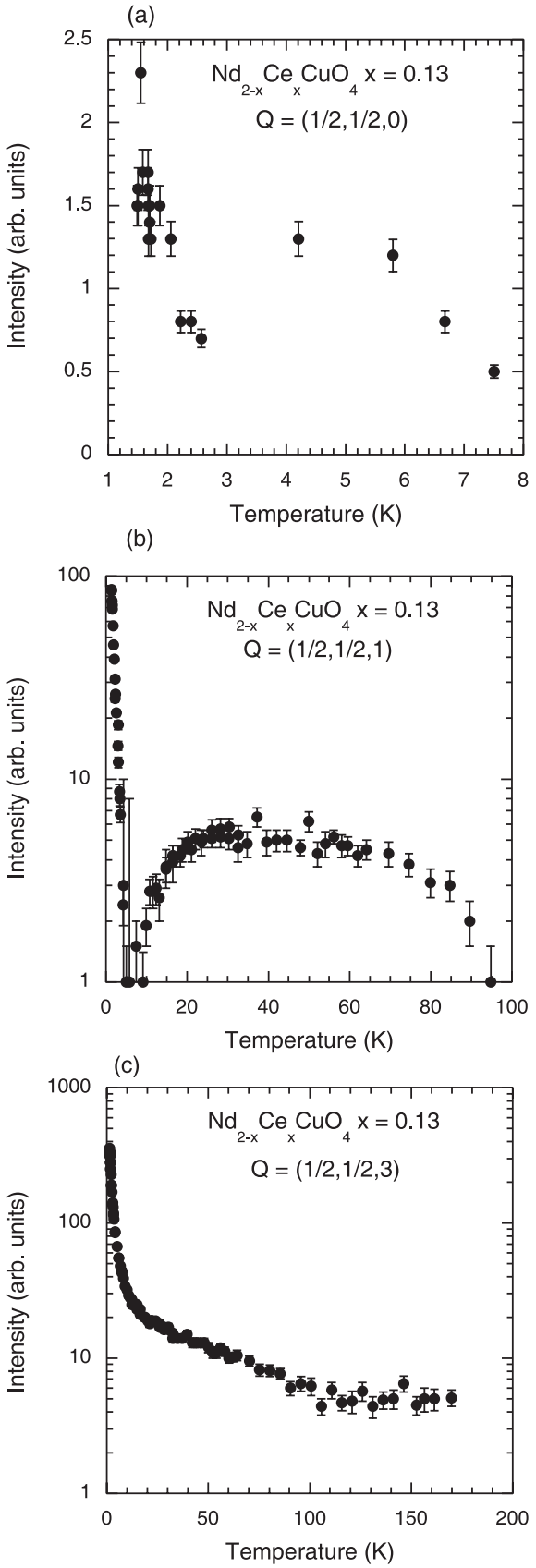

Fig. 3. Temperature variation of the intensities of (a) $\frac{1}{2}\frac{1}{2}0$, (b) $\frac{1}{2}\frac{1}{2}1$ and (c) $\frac{1}{2}\frac{1}{3}3$ reflections of $Nd_{2-x}Ce_xCuO_4$ for $x = 0.13$.

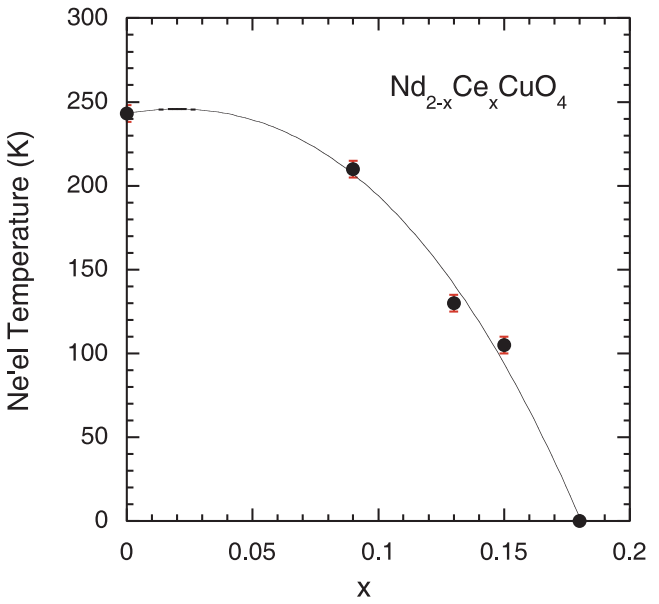

Fig. 4. Variation of the Cu ordering temperature T_N of $Nd_{2-x}Ce_xCuO_4$ as a function of Ce doping x. The continuous line is only a guide to the eyes.

$\mu_\perp$ is the component of the magnetic moment perpendicular to the scattering plane, $f(\mathbf{Q})$ is the magnetic form factor, $\mathbf{Q}$ is the scattering vector, $\mathbf{I}$ is the nuclear spin and $\mathbf{P}$ is an unit vector in the direction of nuclear polarization. The coherent scattering length for the natural Nd atom $b_c = 7.69 \times 10^{-13}$ and $\frac{1}{2}b_N = 0.92 \times 10^{-13}$ cm for the natural Nd atom. Thus the cross sections of the three scattering processes are of the same order of magnitude for natural Nd. One must note the Q dependence of the three scattering processes. The magnetic scattering process is Q dependent through the magnetic form factor $f(\mathbf{Q})$ whereas the two other scattering cross sections are Q independent. Another important difference between the magnetic scattering and the scattering from the polarised nuclear moments is that in the former case only the magnetization component perpendicular to the scarttering vector contribute to the scattering, whereas no such selection rule exists for the latter. In particular if the scattering vector is parallel to the magnetization then the magnetic scattering is zero whereas the scattering from polarized nuclear moments can exist.

The $\frac{1}{2}\frac{1}{2}0$ reflection in Nd_2CuO_4 is a pure nuclear polarization peak and its intensity has a simple relationship to the polarization of the nuclear moments [9]. Figure 5 shows the temperature variation of the intensity of the $\frac{1}{2}\frac{1}{2}0$ reflection of $Nd_{2-x}Ce_xCuO_4$ for $x = 0$, 0.13, 0.15 and 0.18. We have fitted the intensity with the square of the Brilliouin function $B_{I=\frac{7}{2}}(\frac{a_0 I}{T})$

$$F^2 = c\left\{B_{I=\frac{7}{2}}\left(\frac{a_0 I}{T}\right)\right\}^2 + a \qquad (8)$$

where c is a constant of proportionality, a_0 is the hyperfine parameter and I is the nuclear spin and a is the additive

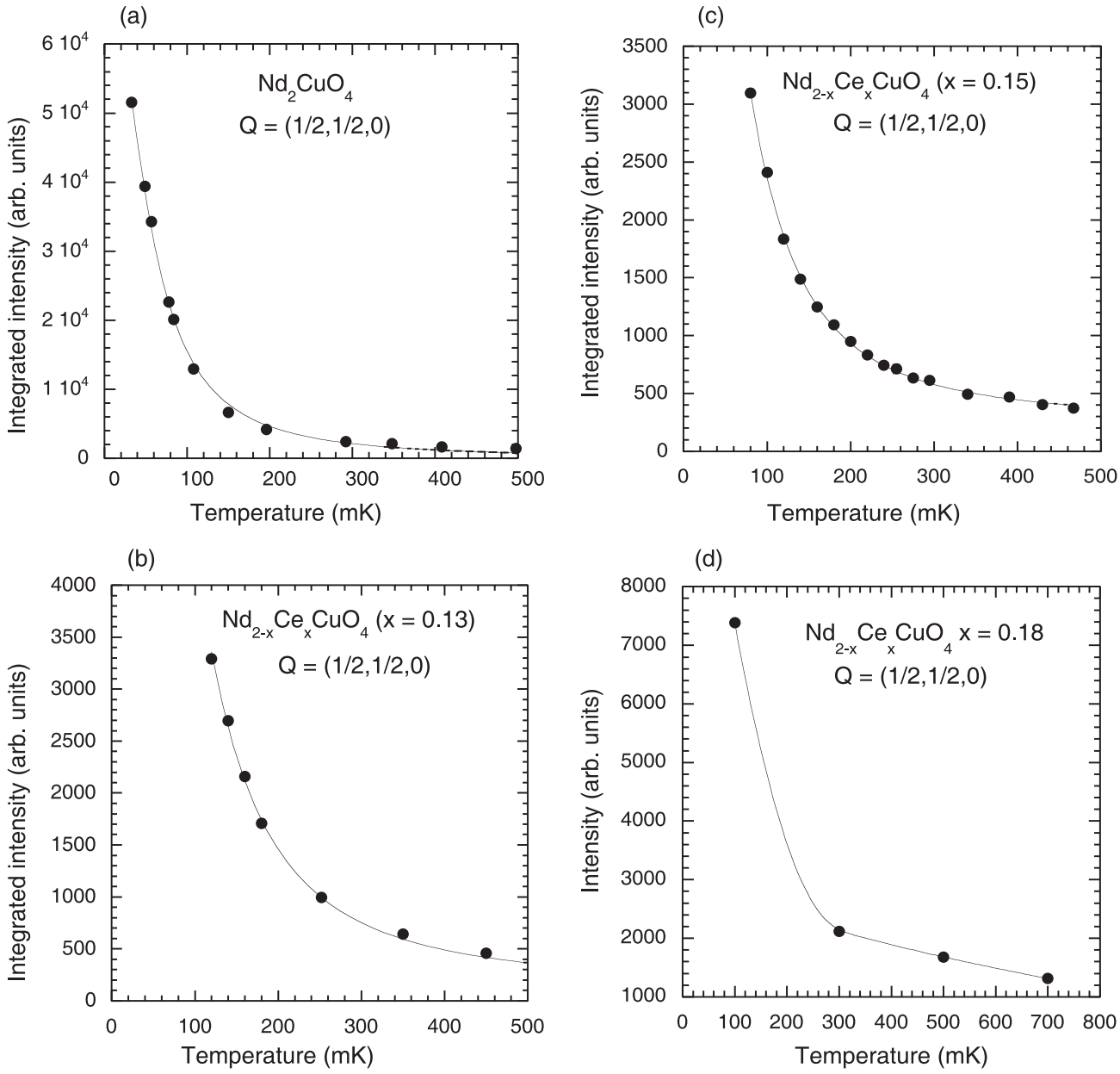

Fig. 5. Temperature variation of the intensity of the $\frac{1}{2}\frac{1}{2}0$ reflection of $Nd_{2-x}Ce_xCuO_4$ for (a) $x = 0$, (b) $x = 0.13$, (c) $x = 0.15$ and (d) $x = 0.18$. We have fitted the temperature variation of the intensities for $x = 0, 0.13, 0.15$ by the square of Brillioiun function given in equation (1) and shown by the continuous lines. The error bars are smaller than the size of the data symbols. We have not attempted to fit the data for the sample with $x = 0.18$ shown in (d). The continuous curve in (d) is just a guide to the eyes.

constant to the intensity due to small higher order wavelength contamination. Least squares fit to these data gave hyperfine parameters $a_0 = 34.6 \pm 0.8, 40 \pm 6, 42 \pm 2$ mK for $x = 0, 0.13$ and 0.15, respectively. We have fitted three parameters: the constant of proportionality c which when the intensity data were in absolute units, could yield the difference $|b^+ - b^-|$, the hyperfine parameter a_0 and an additive constant a to the intensity. b^+ and b^- are the scattering lengths with neutron spins parallel and antiparallel to the nuclear spin. We see that the hyperfine constant a_0 is practically constant within the uncertainty and does not depend very much on the doping. There may be an indication of increase in the hyperfine constant with doping but the large uncertainty in the fit procedure and large standard deviations make this apparent increase doubtful. In any case the hyperfine constant is insensitive to the Ce doping. This is exactly what one expects because upon doping electrons go to the Cu-O plane. The Nd atoms are depleted by the substitution of the Ce atoms but the hyperfine field produced by the electronic moments of the Nd atoms on the nuclear spin remains unchanged on doping.

3.2 Field dependence

We have measured the magnetic field variation of the intensities of $\frac{1}{2}\frac{1}{2}0$, $\frac{1}{2}\frac{1}{2}1$, $\frac{1}{2}\frac{1}{2}2$, $\frac{1}{2}\frac{1}{2}3$, $\frac{1}{2}\frac{1}{2}4$, $\frac{1}{2}\frac{1}{2}5$, $\frac{1}{2}\frac{1}{2}6$ superstructure and the 110 fundamental reflections of Nd_2CuO_4 in fields up to 5 tesla applied parallel to the $[1,-1,0]$ crystallographic direction at $T = 50$ mK, 200 mK, 500 mK and 2 K. We already published [10] some of these results. The superstructure reflections with l = odd decrease continuously and become zero at a critical field of about 0.75 tesla. There exists no significant hysteresis in the field variation of the intensities. The superstructure reflections with even l increase in intensity with increasing magnetic field up to about 0.75 tesla and then decrease with magnetic field up to 5 tesla, the maximum field obtained during the experiment. Figure 6a shows the magnetic field variation of the intensity of the $\frac{1}{2}\frac{1}{2}1$ and $\frac{1}{2}\frac{1}{2}3$ reflections of Nd_2CuO_4. Their intensities decrease continuously and becomes zero at $T_c = 0.75$ tesla. Figure 6b shows the field dependence of the $\frac{1}{2}\frac{1}{2}0$ reflection of Nd_2CuO_4 at $T = 50$ mK and 250 mK. This reflection has no contribution from the electronic magnetic moments and arise purely from nuclear polarisation effects at millikelvin temperatures. The field variation of the intensity of the $\frac{1}{2}\frac{1}{2}0$ reflection at $T = 50$ mK is similar to those of $\frac{1}{2}\frac{1}{2}2$ published by us [10] previously, viz. it increases with increasing magnetic field almost linearly up to the critical field $H_c \approx 0.75$ tesla and then decreases almost linearly. At $T = 250$ mK the intensity of this reflection is reduced very much indicating that the nuclear polarisation is almost absent at that temperature. The intensity of the 110 reflection increases linearly with increasing magnetic field.

These results can be understood by assuming that the application of the magnetic field parallel to $[1,-1,0]$ causes a field-induced double-**k** to single-**k** (or non-collinear to collinear) second-order phase transition at about at $H_c = 0.75$ tesla. The absence of hysteresis in the field variation of the intensity of superstructure reflections confirms that the magnetic structure of both Cu and Nd sublattices at $H = 0$ is double-**k** also at millikelvin temperatures. It should be noted that the superstructure reflections with odd l and with even l belong to the two different propagation vectors of the double-**k** structure. It is because of this that the intensities of the superstructure reflections with odd and even l behave differently as functions of magnetic field, i.e., when one increases in intensity the other decreases and vice versa. The critical field at which the magnetic structure of Nd_2CuO_4 becomes single-**k** or collinear is about 0.7 tesla at $T = 50$, 200 and 500 mK. At $T = 2.0$ K, the highest temperature obtained during the present measurements, the critical field is increased to about 1.0 tesla.

We have already noted that the field dependence of the $\frac{1}{2}\frac{1}{2}0$ reflection is very similar to those of other superstructure reflections with even l. Remembering that this reflection originate purely from the nuclear polarization effect, we conclude that the nuclear spin structure which is also a non-collinear double-**k** type at zero field

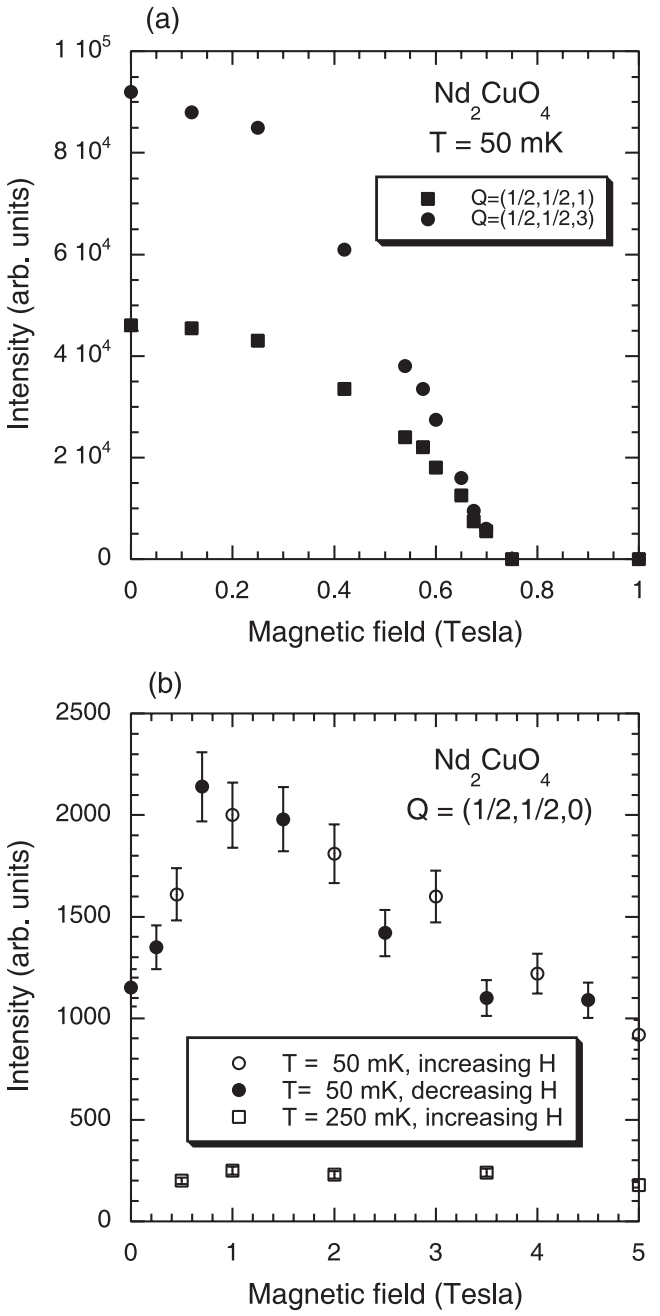

Fig. 6. (a) Magnetic field variation of the intensities of $\frac{1}{2}\frac{1}{2}1$ and $\frac{1}{2}\frac{1}{2}3$ reflections of Nd_2CuO_4 at 50 mK. (b) Magnetic field variation of the intensities of $\frac{1}{2}\frac{1}{2}0$ reflection of Nd_2CuO_4 at 50 and 250 mK. This reflection arises purely from the nuclear polarization effects and has no electronic magnetic contribution. The field dependence of the $\frac{1}{2}\frac{1}{2}0$ reflection is very similar to those of other superstructure reflections with even l [10].

undergoes a similar field-induced double-**k** to single-**k** (or non-collinear to collinear) second-order phase transition at about 0.75 tesla. The intensity of this reflection is reduced almost to zero at 250 mK as expected because the nuclear polarization contribution is very small at this temperature. The 110 structural reflection increases continuously in intensity as the magnetic field is increased. This is due

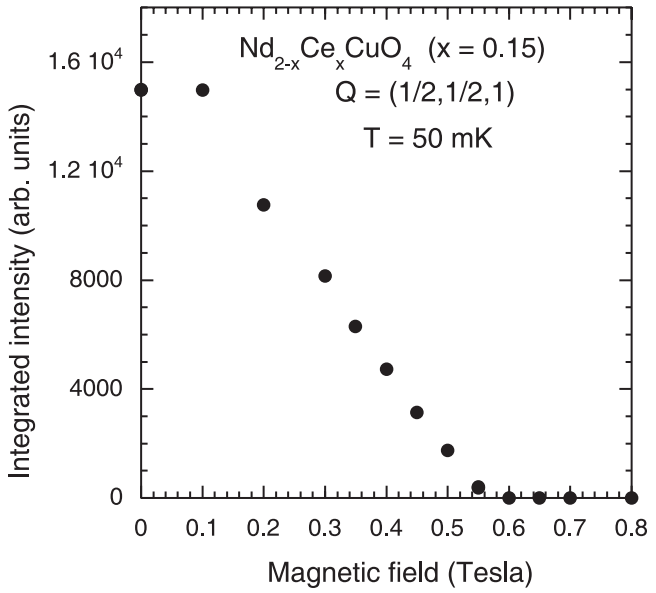

Fig. 7. Magnetic field variation of the intensities of $\frac{1}{2}\frac{1}{2}1$ superlattice reflections of $Nd_{2-x}Ce_xCuO_4$ with $x = 0.15$ at $T = 50$ mK.

to the canting of Nd electronic and nuclear magnetic moments parallel to the field direction. This causes magnetic contribution to the structural 110 reflection.

We have performed similar field-dependent measurements on $Nd_{2-x}Ce_xCuO_4$ with $x = 0.13$ and 0.15. We do not show all the results but discuss here only the results for $x = 0.15$. Figure 7 shows the field variation of the intensities of $\frac{1}{2}\frac{1}{2}1$ superstructure reflections of $Nd_{2-x}Ce_xCuO_4$ with $x = 0.15$ at $T = 50$ mK. The intensity decreases continuously with increasing field and becomes zero at the critical field $H_c \approx 0.56$ tesla. The critical field H_c is shifted towards lower field compared to the undoped sample. Other $\frac{1}{2}\frac{1}{2}l$ reflections with $l =$ odd behave similarly. Figure 8 shows the field variation of the intensity of the $\frac{1}{2}\frac{1}{2}2$ and $\frac{1}{2}\frac{1}{2}0$ reflections. The intensity increases continuously up to $H_c \approx 0.56$ tesla and then decreases continuously. Note that the $\frac{1}{2}\frac{1}{2}0$ reflection originates from pure nuclear polarization effects and has no electronic magnetic contribution. Field variation for other $\frac{1}{2}\frac{1}{2}l$ reflections with $l =$ even is similar. $Nd_{2-x}Ce_xCuO_4$ with $x = 0.15$ shows field induced double-**k** to single-**k** (or non-collinear to collinear) second-order phase transition at $H_c \approx 0.56$ tesla. So the field dependence of the doped samples $Nd_{2-x}Ce_xCuO_4$ is very similar to that of the undoped Nd_2CuO_4. Only the critical field H_c is shifted towards lower field.

The field-induced double-**k** to single-**k** (or non-collinear to collinear) transition has also been observed in Nd_2CuO_4 at higher temperatures at which induced Nd moment is negligible [4]. So the Cu magnetic subsystem also undergoes same phase transition in magnetic field applied parallel to $[1, -1, 1]$ in all the three phases I, II and III. The effect of magnetic field on the superstructure $\frac{1}{2}\frac{1}{2}l$ reflections in phase II is just opposite to those of phases I and II. The superstructure reflections with $l =$ even decreases continuously with field and becomes zero at the critical field H_c whereas the superstructure reflections with $l =$ odd increase at first with increasing field up to H_c and then decrease slowly. Figure 9 shows the temperature variation of the critical field H_c in which we have included higher temperature data from references [4]. The critical field shows a maximum at about $T \approx 25$ K.

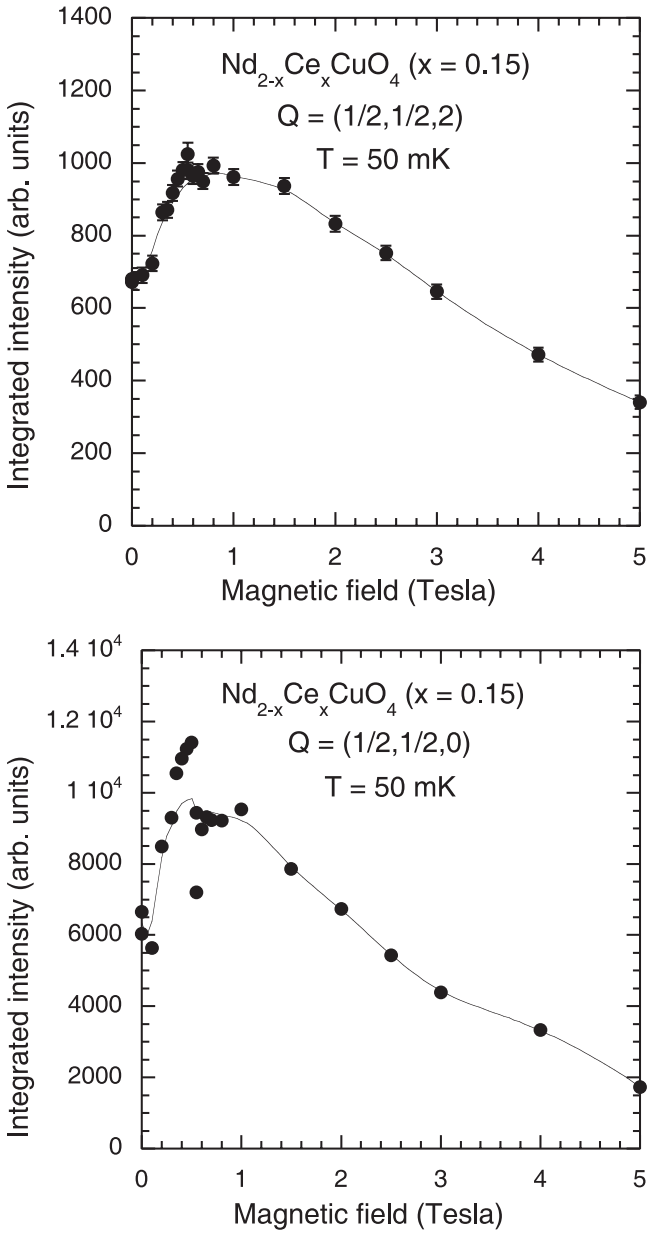

Fig. 8. Magnetic field variation of the intensity of (a) the $\frac{1}{2}\frac{1}{2}2$ and (b) $\frac{1}{2}\frac{1}{2}0$ reflections of $Nd_{2-x}Ce_xCuO_4$ with $x = 0.15$ at $T = 50$ mK. The continuous lines are guides to the eyes.

4 X-ray resonant magnetic scattering

We have done X-ray resonant magnetic scattering investigations on $Nd_{2-x}Ce_xCuO_4$ single crystals for $x = 0$ and 0.15. The mosaic spread of the Nd_2CuO_4 crystal was

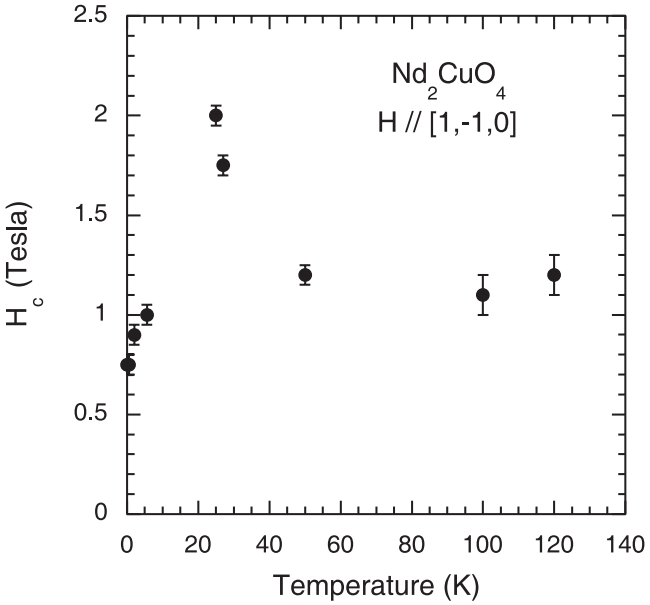

Fig. 9. Temperature variation of the critical field H_c at which double-**k**-single**k** transition takes place. We have included higher temperature data from references [4].

found to be about 0.1 degree. Search for magnetic reflections at low temperatures with X-ray energy tuned to the L_{II} absorption edge of Nd ($E = 6722$ eV) readily revealed magnetic intensities at the reciprocal positions corresponding to to the propagation vector $\mathbf{k} = (\frac{1}{2}, \frac{1}{2}, 0)$. Figure 10a shows the variation of the intensity of $(\frac{1}{2}, \frac{1}{2}, 6)$ magnetic reflection as a function of X-ray energy at $T = 1.9$ K. Figure 10b shows the variation of the background or the fluorescence intensity which is proportional to the absorption. Strong resonance enhancement of the magnetic scattering is observed at the L_{II} absorption edge of Nd. The peak intensity at $E = 6722$ eV was about 30 counts per second at 1.9 K. Figure 11 shows the temperature variation of the intensity of the $(\frac{1}{2}, \frac{1}{2}, 6)$ reflection at $E = 6722$ eV. The intensity of the reflection decreases continuously with temperature but could still be observed at 20 K. The intensity is proportional to the square of the magnetization of the Nd sublattice only, since the contribution due to the Cu sublattice is negligible. The Nd magnetic moments are polarized due to the mean field of the ordered Cu magnetic sublattice. We have fitted the intensity with the square of the Brilliouin function. We have assumed that the magnetic moments are due to the "$S = \frac{1}{2}$" pseudo spins of the lowest CEF Γ_6 doublet of Nd^{3+}. The fitted intensity is shown by the continuous curve in Figure 11. The mean field of the ordered Cu magnetic sublattice on the Nd is found to be 6.2 ± 1.0 K which is about 0.54 ± 0.1 meV. This compares well with the value 0.51 ± 0.2 meV determined by the inelastic neutron scattering investigation of the Nd spin wave dispersion [12]. The present results of the X-ray resonant magnetic scattering agrees well with those reported by Hill et al. [14].

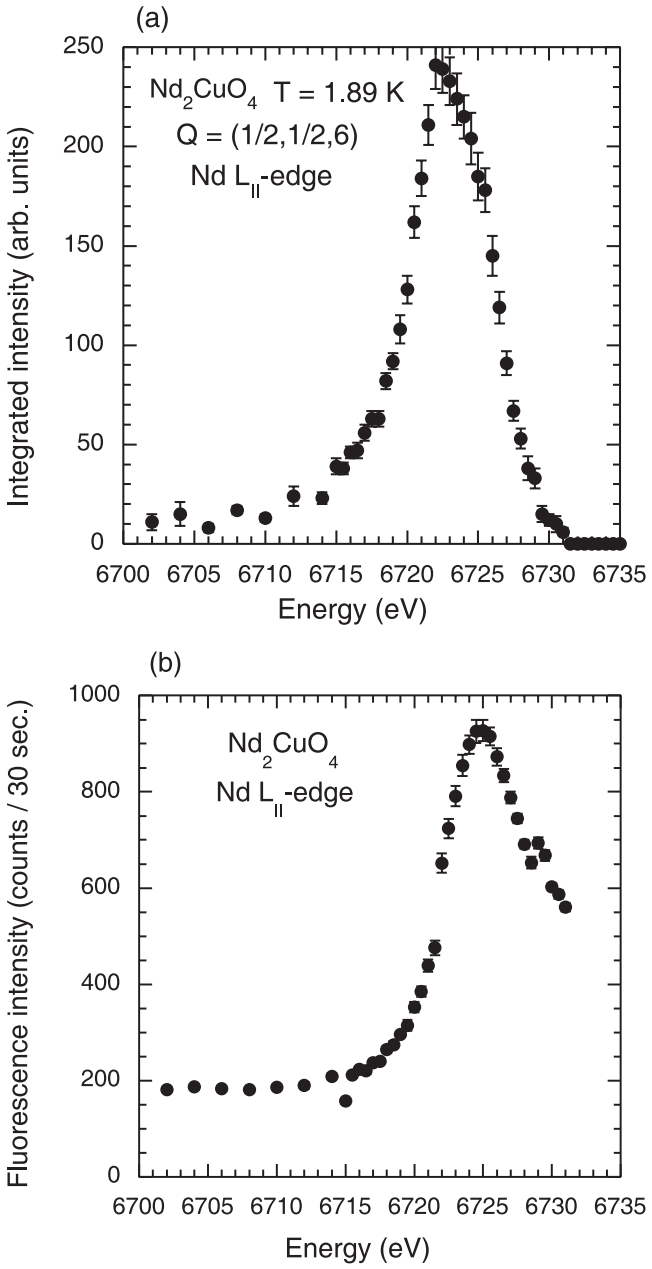

Fig. 10. (a) The variation of the intensity of $(\frac{1}{2}, \frac{1}{2}, 6)$ magnetic reflection of Nd_2CuO_4 as a function of X-ray energy at $T = 1.9$ K. (b) shows the variation of the background or the fluorescence intensity which is proportional to the absorption.

We have performed similar X-ray resonant magnetic scattering investigations on $Nd_{2-x}Ce_xCuO_4$ ($x = 0.15$) single crystal which had a mosaic spread of about 0.04 degree. We readily detected magnetic intensities at reciprocal positions corresponding to the propagation vector $\mathbf{k} = (\frac{1}{2}\frac{1}{2}0)$ at low temperature with the X-ray energy tuned to the L_{II} absorption edge of Nd. Figure 12a shows the variation of the intensity of the $\frac{1}{2}\frac{1}{2}6$ reflection as a function of X-ray energy at $T = 4.35$ K. Figure 12b shows the fluorescence intensity. Strong resonance enhancement of the magnetic scattering is observed in $Nd_{2-x}Ce_xCuO_4$

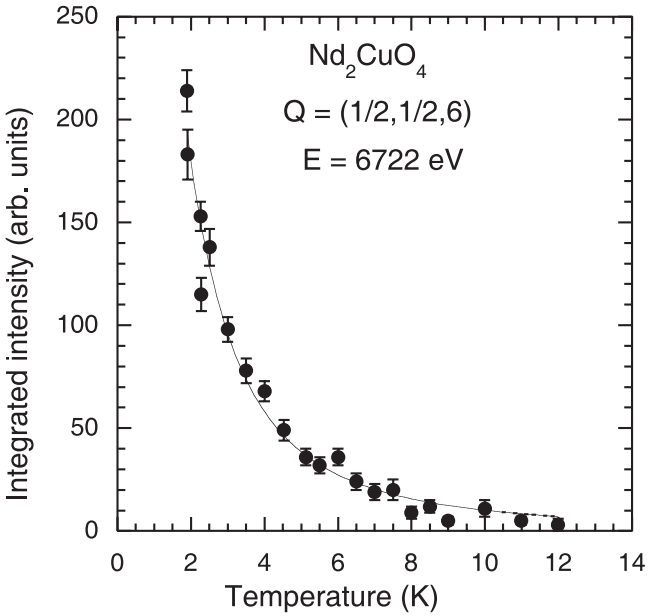

Fig. 11. Temperature variation of the intensity of the $(\frac{1}{2},\frac{1}{2},6)$ reflection of Nd_2CuO_4 at $E = 6722$ eV. The continuous curve is the result of least-squares fit of the data to the square of the Brilliouin function.

($x = 0.15$) at the L_{II} absorption edge of Nd as in the case of the stoichiometric Nd_2CuO_4. Figure 13 shows the temperature variation of the intensity of the $\frac{1}{2}\frac{1}{2}6$ magnetic reflection at $E = 6723$ eV. We have fitted the intensity with the square of the Brilliouin function which is shown by the continuous curve of Figure 13. The mean field of the ordered Cu magnetic sublattice on the Nd is found to be 6.6 ± 0.4 K which is equal to 0.57 ± 0.04 meV. This is of about the same value as determined in stoichiometric Nd_2CuO_4.

Comparison of Figures 2 and 11 will convince one the usefulness of the element-specific X-ray resonance magnetic scattering technique in investigating the magnetic systems with several magnetic sublattices. The temperature variation of the intensity of $\frac{1}{2}\frac{1}{2}1$ reflection obtained by X-ray resonance magnetic scattering at the Nd L_{II} edge (Figs. 11 and 13) is due to the increase of Nd magnetic moment at lower temperature. The relative contribution of magnetic moment of Cu to the intensity of this reflection is negligible for X-ray energies close to the Nd L_{II} edge. The monotonous increase in intensity with decrease of temperature can be fitted by the square of the Brillouin function. The intensity variation of $\frac{1}{2}\frac{1}{2}1$ reflection in neutron diffraction is far more complicated because both Cu and Nd magnetic moments contribute to the intensity of this reflection. We have been able to disentangle the contribution of Nd and Cu moments in this particular case because of the known magnetic structures of the Cu and Nd sublattices and also due to the fact that Cu magnetic moment is fully saturated at low temperatures. In general it is more difficult to analyze the magnetic structures with several sublattices by neutron diffraction. The element specific X-ray resonance magnetic scattering is very

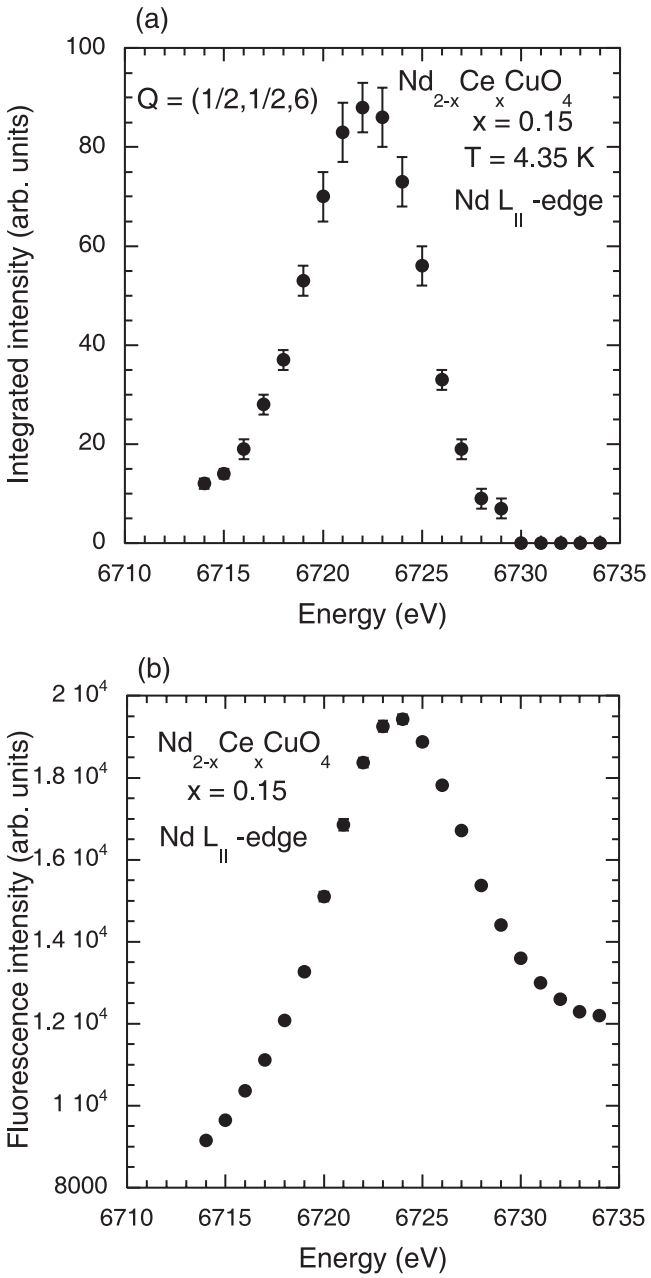

Fig. 12. (a) The variation of the intensity of $(\frac{1}{2},\frac{1}{2},6)$ magnetic reflection of $Nd_{2-x}Ce_xCuO_4$ with $x = 0.15$ as a function of X-ray energy at $T = 4.35$ K. (b) shows the variation of the background or the fluorescence intensity which is proportional to the absorption.

useful in determining the magnetic structures with several magnetic sublattices. However, the best strategy in such cases is to combine neutron and X-ray resonance magnetic scattering techniques.

5 Discussion

The pure Nd_2CuO_4 and the doped $Nd_{2-x}Ce_xCuO_4$, apart from being interesting materials related to high-T_c superconductivity, represent a very interesting magnetic system

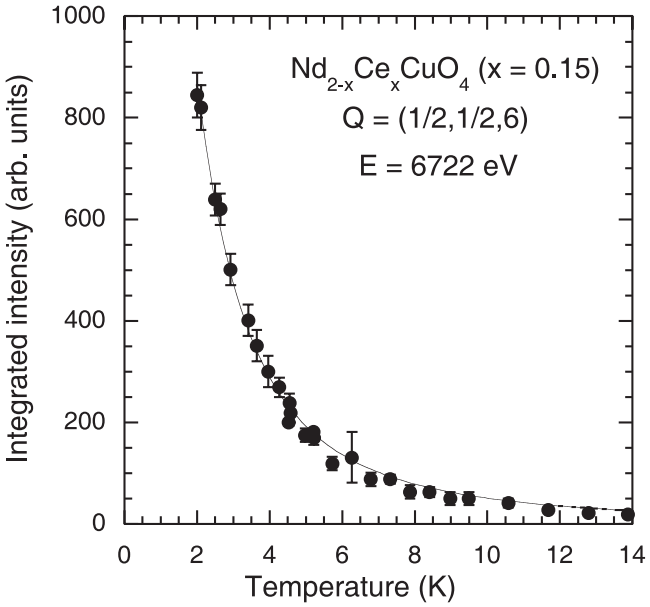

Fig. 13. Temperature variation of the intensity of the $(\frac{1}{2},\frac{1}{2},6)$ reflection of $Nd_{2-x}Ce_xCuO_4$ with $x = 0.15$ at $E = 6722$ eV. The continuous curve is the result of least-squares fit of the data to the square of the Brilliouin function.

with several magnetic sublattices. The undoped parent compound together with the other members of the general formula R_2CuO_4 where R is a lanthanide, is described as Mott-Hubbard insulators. They exhibit an antiferromagnetic ordering below a Néel temperature T_N which ranges between 240 and 320 K. There exist three magnetic sublattices: the Cu and the Nd electronic magnetic sublattices and the Nd nuclear magnetic sublattice. There also exist several energy scales involving these sublattices. (1) A very strong in plane Cu-Cu exchange interaction, which is actually due to the Cu-O-Cu superexchange interaction. This interaction has been determined by inelastic neutron scattering investigations of the spin wave dispersion below T_N and has been found to be 155 ± 3 meV [15]. A very small interplanar Cu-Cu interaction leads to the three dimensional magnetic ordering of the Cu magnetic moments at $T_N \approx 240$ K. The strong Cu-Cu interaction leads to two-dimensional correlation in the Cu-O plane which is observed in the neutron scattering experiments as rods of diffuse scattering at temperatures as high as 500 K. The width of this rod is a direct measure of the inverse correlation length. In the temperature range $T_N < T \leq 500$ K the system behaves as a 2D $S = \frac{1}{2}$ quantum Heisenberg antiferromagnet. Analytical results are not yet available for this model, but approximate theoretical methods and simulations have been employed to calculate spin-spin correlation length as function of temperature [16]. The 2D spin correlations within the CuO layer develop progressively with decreasing temperature. A crossover to 3D behavior takes place when the interplanar coupling between the correlated regions become of the order of kT. (2) We consider next the Nd-Cu interaction. The dominant Nd-Cu are those between nearest neighboring Nd and Cu planes. The interaction cannot be the usual isotropic exchange interaction, because in that case the exchange field on a Nd ion when summed over the neighboring Cu ions would vanish. It is therefore necessary to introduce a pseudodipolar interaction which results from the anisotropic component of the Nd-Cu exchange interaction [17]. This interaction produces a staggered magnetic field of about 0.5 meV at the Nd ion in undoped Nd_2CuO_4. (3) The Nd-Nd interaction causes Nd spin wave dispersion and have been determined by inelastic neutron scattering. These interactions lie in the range from 4 μeV to 33 μeV [11]. (4) Finally the hyperfine induced polarization of the ^{143}Nd and ^{145}Nd isotopes with nuclear spin $I = 7/2$ is to be considered at millikelvin temperatures [9,18,19].

The magnetic ordering, non-collinear spin structure, spin reorientation phase transitions and other low temperature magnetic properties of pure Nd_2CuO_4 can be understood by invoking the four types of magnetic interactions described above. Most of the magnetic properties of Nd_2CuO_4 are mainly due to the coupling between the Cu and the Nd subsystem which exhibits a large single ion anisotropy. According to Sachidanadandam et al. [17] this anisotropy together with a pseudodipolar interaction arising from the anisotropy of the Nd-Cu exchange stabilizes the magnetic structure. The spin reorientation transitions in Nd_2CuO_4 have been explained by Sachidanadandam et al. [17] in terms of a competition between the various interplanar interactions which arise because of the rapid temperature dependence of the Nd moment below about 100 K. Below about 10 K Nd-Nd interactions become increasingly important and must be invoked to explain Nd spin waves. Below about 1 K the hyperfine interaction [9,18,19] between the Nd electronic and nuclear moments become important and should be considered for understanding magnetic properties of Nd_2CuO_4 in millikelvin temperatures.

Our experimental results on $Nd_{2-x}Ce_xCuO_4$ suggests that on doping with Ce, although the the magnetic properties of the Cu subsystem changes drastically, Nd subsystem is not very sensitive. The Néel temperature or the Cu ordering temperature of $Nd_{2-x}Ce_xCuO_4$ decreases continuously with doping. For $x = 0.18$ the Cu subsystem does not show any long range order but the Nd sublattice becomes ordered at low temperature as is clearly seen by the temperature variation of the $(\frac{1}{2},\frac{1}{2},1)$ reflection. The temperature dependence of the intensity of the $(\frac{1}{2},\frac{1}{2},1)$ reflection of $Nd_{2-x}Ce_xCuO_4$ for $x = 0.18$ has a shape which indicates induced ordering. But induced ordering of Nd sublattice is not possible when the Cu sublattice is not ordered. This apparent contradiction can be resolved by assuming that some sort of Cu magnetic order still persists for $x = 0.18$. We failed to detect magnetic ordering of $Nd_{2-x}Ce_xCuO_4$ for $x = 0.18$, but we cannot rule it out if the magnetic moment becomes smaller than the limit of detection by neutron diffraction. The detection of the Cu magnetic ordering can be difficult if the magnetic correlation length is substantially reduced. The detection of Nd magnetic ordering is easier due to the larger magnetic moment involved. More

systematic investigation of the influence of the Ce-doping on the magnetic ordering of $Nd_{2-x}Ce_xCuO_4$ has been done by Lynn and coworkers [4]. They have constructed the (T, x) phase diagram of $Nd_{2-x}Ce_xCuO_4$ that shows the regions of superconducting (SC), antiferromagnetic order (AF) and paramagnetic (P) behaviour. The spin reorientation transition temperatures have been shown also. Our results agree with these investigations. They have found no magnetic long range ordering of the Cu sublattice already for the superconducting $Nd_{2-x}Ce_xCuO_{4-y}$ sample with $x = 0.15$. However, the Nd sublattice orders at a well-defined $T_N \approx 1.2$ K. In Ce-doped superconducting samples the Cu spin system is not magnetically ordered, and there is no average staggered field at the Nd site to induce Nd spins to order at higher temperature. Hence the magnetic ordering of Nd moments is spontaneous. However, this superconducting sample was reduced in oxygen and differs from that of our $Nd_{2-x}Ce_xCuO_4$ with $x = 0.15$. Lynn and coworkers [4] concluded that there exist no long-range magnetic ordering of either Cu or Nd for $Nd_{2-x}Ce_xCuO_4$ samples with $x \geq 0.17$. We admit that we have not done any extensive investigation of the magnetic ordering for the $Nd_{2-x}Ce_xCuO_4$ sample with $x = 0.18$. The intensity of the magnetic reflections for the sample with $x = 0.18$ was very small and limited neutron beam time did not allow us extensive investigation of this sample.

The spin reorientation transitions persist in $Nd_{2-x}Ce_xCuO_4$ for $x \leq 0.15$. But on doping the spin reorientation transitions are not any more sharp phase transitions, but are broad. The Nd ordering is more or less unaffected on doping. The hyperfine-induced nuclear polarization is also insensitive to doping with Ce.

Thalmeier [20] has explained theoretically the field-induced non-collinear to collinear phase transition in Nd_2CuO_4 at $H_c = 0.75$ tesla. He has described this transition within an exchange model for the Cu and Nd moments. The exchange model has been determined by zero-field inelastic neutron scattering investigations [11]. The critical field is temperature dependent as is shown in Figure 9. The phase transition takes place at all temperatures below T_N and in all three magnetic phases I, II and III of Nd_2CuO_4. The critical field H_c which is 0.75 tesla at 50 mK increases at first with increasing temperature, has a maximum of about $H_c \approx 2$ tesla at $T = 25$ K. H_c is then reduced with temperature and becomes about $H_c \approx 1.2$ tesla at $T = 120$ K. According to Thalmeier [20] the phase transition is caused by the Cu-Cu exchange anisotropy. At higher temperatures at which there is no ordered Nd moment, only the Cu moments turn and tilt. At lower temperatures, due to the considerable Cu-Nd exchange field of the order of 0.5 meV, Nd sublattice co-rotate with the Cu moments in the field. Temperature dependence of the critical field H_c is perhaps a result of the competition between the strengths of the above mentioned interactions which are sensitive functions of temperature. Below about 400 mK the polarized Nd nuclear sublattice also co-rotate with the Cu and Nd electronic sublattice with magnetic field applied along $[1, -1, 0]$ to produce a field-induced double-**k** to single-**k** or non-collinear to collinear phase transition. Since the Cu-Nd exchange field reduces with Ce doping the critical field H_c for this transition in Ce-doped samples is reduced.

6 Summary and conclusions

We have determined the magnetic ordering of Cu and Nd electronic magnetic subsystems and also hyperfine induced polarization of Nd nuclear magnetic moments of Nd_2CuO_4 and $Nd_{2-x}Ce_xCuO_4$ by neutron diffraction and resonant X-ray magnetic scattering at zero applied magnetic field in the temperature range from 250 K down to about 33 mK and also their field dependence at millikelvin temperatures up to 5 tesla. We have shown that the increase of intensity of the superlattice reflections below about 400 mK to be due to hyperfine induced polarization of the Nd nuclear magnetic moments. The electronic magnetic ordering and the spin reorientation transition in $Nd_{2-x}Ce_xCuO_4$ strongly depends on Ce doping whereas the hyperfine coupling constant is nearly independent of doping. The field-induced continuous double-**k** to single-**k** transition from the non-collinear to the collinear magnetic structure has been investigated. The critical field H_c for this transition depends strongly on both temperature and doping with Ce.

In conclusion we have shown that most of the low temperature magnetic properties of Nd_2CuO_4 and $Nd_{2-x}Ce_xCuO_4$ can be understood by invoking the four types of interactions involving Cu-Cu, Cu-Nd, Nd-Nd and hyperfine interaction between Nd electronic and nuclear magnetic moments. We have established that (a) nuclear polarisation of the Nd nuclear moments play an important role in determining the magnetic properties of $Nd_{2-x}Ce_xCuO_4$ at millikelvin temperatures and (b) the magnetic field induced phase transition from the non-collinear double-**k** to the single-**k** collinear structure takes place not only for the Cu and Nd sublattices but also for the polarised nuclear magnetic structure at millikelvin temperatures.

We thank Dr. P. Thalmeier, Dr. P.J. Brown for critical discussions. The experiments at BENSC and HASYLAB were supported by the European Commission.

References

1. Y. Tokura, H. Takagi, S. Uchida, Nature **337**, 345 (1989)
2. R.J. Gooding, K.F.E. Vos, P.W. Leung, Phys. Rev. B **50**, 12866 (1994), and the references therein
3. M. Matsuda, K. Yamada, K. Kakurai, H. Kadowaki, T.R. Thurston, Y. Endoh, Y. Hidaka, R.J. Birgeneau, M.A. Kastner, P.M. Gehring, A.H. Moudden, G. Shirane, Phys. Rev. B **42**, 10098 (1990); Phys. Rev. B **45**, 12548 (1992)
4. S. Skanthakumar, Ph.D. thesis, University of Maryland (1993)

5. S. Skanthakumar, H. Zhang, T.W. Clinton, W.-H. Li, J.W. Lynn, Z. Fisk, S.-W. Cheong, Physica C **160**, 124 (1989); J.W. Lynn, I.W. Summerlin, S. Skanthakumar, W.-H. Li, R.N. Shelton, J.L. Peng, Z. Fisk, S.-W. Cheong, Phys. Rev. B **41**, 2569 (1990)
6. D. Petitgrand, A.H. Moudden, P. Galez, P. Boutrouille, J. Less Comm. Met. **164 & 165**, 768 (1990)
7. P. Allenspach, S.-W. Cheong, A. Dommann, P. Fischer, Z. Fisk, A. Furrer, H.R. Ott, B. Rupp, Z. Phys. B **77**, 185 (1989)
8. T. Chattopadhyay, P.J. Brown, U. Köbler, Physica C **177**, 294 (1991)
9. T. Chattopadhyay, K. Siemensmeyer, Europhys. Lett. **29**, 579 (1995)
10. T. Chattopadhyay, K. Siemensmeyer, H. Schneider, Physica B **234-236**, 715 (1997)
11. W. Henggeler, T. Chattopadhyay, B. Roessli, P. Vorderwisch, P. Thalmeier, D.I. Zhigunov, S.N. Barilo, A. Furrer, Phys. Rev. B **55**, 1269 (1997)
12. W. Henggeler, B. Roessli, A. Furrer, P. Vorderwisch, T. Chatterji, Phys. Rev. Lett. **80**, 1300 (1998)
13. W. Henggeler, T. Chattopadhyay, P. Thalmeier, P. Vorderwisch, A. Furrer, Europhys. Lett. **34**, 537 (1996)
14. J.P. Hill, A. Vigilante, D. Gibbs, J.L. Peng, R.L. Green, Phys. Rev. B **52**, 6575 (1995)
15. P. Bourges, H. Casalta, A.S. Ivanov, D. Petitgrand, Phys. Rev. Lett. **79**, 4906 (1997)
16. For a theoretical review of the 2D $S = \frac{1}{2}$ quantum antiferromagnet, see E. Manousakis, Rev. Mod. Phys. **63**, 1 (1991)
17. R. Sachidanandam, T. Yildirim, A.B. Harris, A. Aharony, O. Entin-Wohlman, Phys. Rev. B **56**, 260 (1997)
18. W. Marti, M. Medarde, S. Rosenkranz, P. Fischer, A. Furrer, C. Klemenz, Phys. Rev. B **52**, 4275 (1995)
19. J. Bartolomé, E. Palacios, M.D. Kuzmín, F. Bartolomé, I. Sosnowska, R. Przenioslo, R. Sonntag, M.M. Lukina, Phys. Rev. B **55**, 11432 (1997)
20. P. Thalmeier, Physica B **252**, 295 (1998)